Applied Numerical Mathematics 121 (2017) 234–248

Contents lists available at ScienceDirect

Applied Numerical Mathematics

www.elsevier.com/locate/apnum

# Construction of IMEX DIMSIMs of high order and stage order

Z. Jackiewicz [a,b], H. Mittelmann [a,*]

[a] School of Mathematical & Statistical Sciences, Arizona State University, Tempe, AZ 85287, United States
[b] AGH University of Science and Technology, Kraków, Poland

ARTICLE INFO

*Article history:*
Received 7 November 2015
Received in revised form 17 January 2017
Accepted 17 July 2017
Available online 26 July 2017

*Keywords:*
IMEX methods
General linear methods
DIMSIMs
Stability analysis
Optimization methods
Construction of highly stable methods

ABSTRACT

For many systems of differential equations modeling problems in science and engineering, there are often natural splittings of the right hand side into two parts, one of which is non-stiff or mildly stiff, and the other part is stiff. Such systems can be efficiently treated by a class of implicit–explicit (IMEX) diagonally implicit multistage integration methods (DIMSIMs), where the stiff part is integrated by implicit formula, and the non-stiff part is integrated by an explicit formula. We analyze stability of these methods when the implicit and explicit parts interact with each other. We look for methods with large absolute stability region, assuming that the implicit part of the method is $A(\alpha)$-, $A$-, or $L$-stable. Finally, we furnish examples of IMEX DIMSIMs of order $p = 5$ and $p = 6$ and stage order $q = p$, with good stability properties. Numerical examples illustrate that the IMEX schemes constructed in this paper do not suffer from order reduction phenomenon for some range of stepsizes.



## 1. Introduction

Many practical problems in science and engineering are modeled by large systems of ordinary differential equations (ODEs) which arise from discretization in space of partial differential equations (PDEs) by finite difference methods, finite elements or finite volume methods, or pseudospectral methods. For such systems there are often natural splittings of the right hand sides of the differential systems into two parts, one of which is non-stiff or mildly stiff, and suitable for explicit time integration, and the other part is stiff, and suitable for implicit time integration. Such systems can be written in the form

$$\begin{aligned} &y'(t) = f\big(y(t)\big) + g\big(y(t)\big), \quad t \in [t_0, T], \\ &y(t_0) = y_0 \in \mathbb{R}^m, \end{aligned} \tag{1.1}$$

where $f(y)$ represents the non-stiff processes, for example advection, and $g(y)$ represents stiff processes, for example diffusion or chemical reaction, in semidiscretization of advection–diffusion–reaction equations [21].

As in [1,35,14] consider the transformation $y = x + z$, where

$$x' = f(x + z), \tag{1.2}$$

$$z' = g(x + z). \tag{1.3}$$

* Corresponding author.
*E-mail addresses:* jackiewicz@asu.edu (Z. Jackiewicz), mittelmann@asu.edu (H. Mittelmann).

http://dx.doi.org/10.1016/j.apnum.2017.07.004
0168-9274/

In this paper we will analyze methods, where the non-stiff part (1.2) is treated by the explicit DIMSIMs, a subclass of general linear methods (GLMs), with the coefficients $\mathbf{c} = [c_1, \ldots, c_s]^T \in \mathbb{R}^s$,

$$\mathbf{A} = [a_{ij}] \in \mathbb{R}^{s\times s},\ \mathbf{U} = [u_{ij}] \in \mathbb{R}^{s\times r},\ \mathbf{B} = [b_{ij}] \in \mathbb{R}^{r\times s},\ \mathbf{V} = [v_{ij}] \in \mathbb{R}^{r\times r},$$

$a_{ij} = 0$, $j \geq i$, and the stiff part (1.3) is treated by the diagonally implicit DIMSIMs with the coefficients $\mathbf{c} = [c_1, \ldots, c_s]^T \in \mathbb{R}^s$,

$$\widehat{\mathbf{A}} = [\widehat{a}_{ij}] \in \mathbb{R}^{s\times s},\ \mathbf{U} = [u_{ij}] \in \mathbb{R}^{s\times r},\ \widehat{\mathbf{B}} = [\widehat{b}_{ij}] \in \mathbb{R}^{r\times s},\ \mathbf{V} = [v_{ij}] \in \mathbb{R}^{r\times r},$$

$\widehat{a}_{ij} = 0$, $j > i$, $\widehat{a}_{ii} = \lambda$, $i = 1, 2, \ldots, s$, where both methods have the same abscissa vector $\mathbf{c}$ and the coefficient matrices $\mathbf{U}$ and $\mathbf{V}$. The explicit method applied to (1.2) on the grid $t_n = t_0 + nh$, $n = 0, 1, \ldots, N$, $Nh = T - t_0$ takes the form

$$\begin{aligned} X_i^{[n+1]} &= h\sum_{j=1}^{i-1} a_{ij} f\big(X_j^{[n+1]} + Z_j^{[n+1]}\big) + \sum_{j=1}^{r} u_{ij} x_j^{[n]}, \quad i = 1, 2, \ldots, s, \\ x_i^{[n+1]} &= h\sum_{j=1}^{s} b_{ij} f\big(X_j^{[n+1]} + Z_j^{[n+1]}\big) + \sum_{j=1}^{r} v_{ij} x_j^{[n]}, \quad i = 1, 2, \ldots, r, \end{aligned} \tag{1.4}$$

$n = 0, 1, \ldots, N-1$. Similarly, the implicit method applied to (1.3) takes the form

$$\begin{aligned} Z_i^{[n+1]} &= h\sum_{j=1}^{i} \widehat{a}_{ij} g\big(X_j^{[n+1]} + Z_j^{[n+1]}\big) + \sum_{j=1}^{r} u_{ij} z_j^{[n]}, \quad i = 1, 2, \ldots, s, \\ z_i^{[n+1]} &= h\sum_{j=1}^{s} \widehat{b}_{ij} g\big(X_j^{[n+1]} + Z_j^{[n+1]}\big) + \sum_{j=1}^{r} v_{ij} z_j^{[n]}, \quad i = 1, 2, \ldots, r, \end{aligned} \tag{1.5}$$

$n = 0, 1, \ldots, N-1$. Combining (1.4) and (1.5) leads to the class of so-called implicit–explicit (IMEX) DIMSIMs defined by

$$\begin{aligned} Y_i^{[n+1]} &= h\sum_{j=1}^{i-1} a_{ij} f\big(Y_j^{[n+1]}\big) + h\sum_{j=1}^{i} \widehat{a}_{ij} g\big(Y_j^{[n+1]}\big) + \sum_{j=1}^{r} u_{ij} y_j^{[n]},\ i = 1, 2, \ldots, s, \\ y_i^{[n+1]} &= h\sum_{j=1}^{s} \Big(b_{ij} f\big(Y_j^{[n+1]}\big) + \widehat{b}_{ij} g\big(Y_j^{[n+1]}\big)\Big) + \sum_{j=1}^{r} v_{ij} y_j^{[n]}, \quad i = 1, 2, \ldots, r, \end{aligned} \tag{1.6}$$

$n = 0, 1, \ldots, N-1$, where

$$Y_i^{[n+1]} = X_i^{[n+1]} + Z_i^{[n+1]}, \quad y_i^{[n]} = x_i^{[n]} + z_i^{[n]}.$$

It was proved in [35] that if the explicit and implicit method has order $p$ and stage order $q = p$ or $q = p-1$, then the overall method (1.6) has also order $p$ and stage order $q = p$ or $q = p-1$. This means that $X_i^{[n+1]}$ and $Z_i^{[n+1]}$ are approximations of stage order $q$ to $x(t_n + c_i h)$ and $z(t_n + c_i h)$, respectively, i.e.,

$$X_i^{[n+1]} = x(t_n + c_i h) + O(h^{q+1}), \quad Z_i^{[n+1]} = z(t_n + c_i h) + O(h^{q+1}), \tag{1.7}$$

and $x_i^{[n]}$ and $z_i^{[n]}$ are approximations of order $p$ to the linear combinations of the derivatives of the solutions $x$ and $z$ at the point $t_n$, i.e.,

$$x_i^{[n]} = \sum_{k=0}^{p} q_{ik} h^k x^{(k)}(t_n) + O(h^{p+1}), \quad z_i^{[n]} = \sum_{k=0}^{p} \widehat{q}_{ik} h^k z^{(k)}(t_n) + O(h^{p+1}), \tag{1.8}$$

where $x$ and $z$ are solutions to (1.2) and (1.3), and $q_{ik}$, $\widehat{q}_{ik}$ are scalar coefficients. It follows from stage order conditions that $q_{ik}$, $\widehat{q}_{ik}$ are components of the vectors $\mathbf{q}_k$, $\widehat{\mathbf{q}}_k$ defined by

$$\mathbf{q}_0 = \mathbf{e}, \quad \mathbf{q}_k = \frac{\mathbf{c}^k}{k!} - \frac{\mathbf{A}\mathbf{c}^{k-1}}{(k-1)!}, \quad k = 1, 2, \ldots, p, \tag{1.9}$$

$$\widehat{\mathbf{q}}_0 = \mathbf{e}, \quad \widehat{\mathbf{q}}_k = \frac{\mathbf{c}^k}{k!} - \frac{\widehat{\mathbf{A}}\mathbf{c}^{k-1}}{(k-1)!}, \quad k = 1, 2, \ldots, p, \tag{1.10}$$

$\mathbf{e} = [1, 1, \ldots, 1]^T \in \mathbb{R}^s$, compare [35].

Many other classes of IMEX methods were already investigated in the literature on the subject. IMEX Runge–Kutta (RK) were analyzed by Ascher et al. [1], Kennedy and Carpenter [24,25], Zhong [37], García-Celayeta et al. [17] (in a more general context of additive RK methods), Hundsdorfer and Verwer [21], Pareshi and Russo [28,29], Boscarino [3,4], Boscarino and

Russo [7], Boscarino et al. [6,5], Cardone et al. [13], and Izzo and Jackiewicz [22]. IMEX linear multistep methods were introduced by Crouzeix [15] and Varah [31] and further investigated by Ascher et al. [2], Ruuth [30], Frank et al. [16], Hundsdorfer and Verwer [21], Hundsdorfer and Ruuth [20], and Wang and Ruuth [32]. IMEX two-step Runge–Kutta (TSRK) methods were investigated by Zharovsky et al. [36]. Some classes of IMEX GLMs were analyzed by Zhang and Sandu [34], Zhang et al. [35], and Cardone et al. [12,14]. IMEX GLMs with inherent Runge–Kutta stability were analyzed by Braś et al. [8].

The organization of this paper is as follows. In Section 2 we review the stability theory of IMEX DIMSIMs with respect to the test equation with two complex parameters corresponding to the non-stiff and stiff parts of the system (1.1). In Section 3 we describe the construction of IMEX methods with large regions $\mathcal{S}_\alpha$ for $\alpha \in (0, \pi/2]$ assuming that the implicit part of the IMEX scheme is $A(\alpha)$-, $A$-, or $L$-stable. Examples of IMEX DIMSIMs of order $p = 5$ and $p = 6$ are then presented in Sections 3.1 and 3.2. The construction of starting and finishing procedures is described in Section 4. The results of numerical experiments are given in Section 5. Finally, in Section 6 some concluding remarks are given.

## 2. Stability analysis of IMEX DIMSIMs

Similarly as in [34,35,12–14] to analyze the stability properties of IMEX DIMSIMs (1.6) we will use the test equation

$$y'(t) = \lambda_0 y(t) + \lambda_1 y(t), \quad t \geq 0, \tag{2.1}$$

where $\lambda_0$ and $\lambda_1$ are complex parameters corresponding to the non-stiff part and the stiff part of the system (1.1). Applying (1.6) to (2.1) we obtain

$$Y^{[n+1]} = (z_0\mathbf{A} + z_1\widehat{\mathbf{A}})Y^{[n+1]} + \mathbf{U}y^{[n]}, \quad y^{[n+1]} = (z_0\mathbf{B} + z_1\widehat{\mathbf{B}})Y^{n+1]} + \mathbf{V}y^{[n]},$$

$n = 0, 1, \ldots$, where $z_0 = h\lambda_0$, $z_1 = h\lambda_1$. Since we have $\det(\mathbf{I} - z_0\mathbf{A} - z_1\widehat{\mathbf{A}}) \neq 0$, this is equivalent to the vector recurrence relation

$$y^{[n+1]} = \mathbf{M}(z_0, z_1)y^{[n]}, \tag{2.2}$$

$n = 0, 1, \ldots$, with the stability matrix $\mathbf{M}(z_0, z_1)$ defined by

$$\mathbf{M}(z_0, z_1) = \mathbf{V} + (z_0\mathbf{B} + z_1\widehat{\mathbf{B}})(\mathbf{I} - z_0\mathbf{A} - z_1\widehat{\mathbf{A}})^{-1}\mathbf{U}. \tag{2.3}$$

We also define the stability function $p(w, z_0, z_1)$ of the IMEX scheme (1.6) as the stability polynomial of $\mathbf{M}(z_0, z_1)$, i.e.,

$$p(w, z_0, z_1) = \det\big(w\mathbf{I} - \mathbf{M}(z_0, z_1)\big). \tag{2.4}$$

To investigate the stability properties of (1.6) it is usually more convenient to work with the polynomial $(1 - \lambda z_1)^s p(w, z_0, z_1)$, where $\lambda$ is the diagonal element of the coefficient matrix $\widehat{\mathbf{A}}$. This polynomial will be denoted by the same symbol $p(w, z_0, z_1)$.

We say that the IMEX DIMSIM (1.6) is stable for given $z_0, z_1 \in \mathbb{C}$ if all the roots $w_i(z_0, z_1)$, $i = 1, 2, \ldots, r$, of the stability function $p(w, z_0, z_1)$ are inside of the unit circle. In this paper we will be mainly interested in IMEX schemes which are $A(\alpha)$-, $A$-, or $L$-stable with respect to the implicit part $z_1 \in \mathbb{C}$. To investigate such methods we consider, similarly as in [12,13,21,35], the sets

$$\mathcal{S}_\alpha = \Big\{ z_0 \in \mathbb{C} : \text{ the IMEX DIMSIM is stable for any } z_1 \in \mathcal{A}_\alpha \Big\},$$

where the set $\mathcal{A}_\alpha \subset \mathbb{C}$ is defined by

$$\mathcal{A}_\alpha = \Big\{ z \in \mathbb{C} : \ \mathrm{Re}(z) < 0 \quad \text{and} \quad |\mathrm{Im}(z)| \leq \tan(\alpha)|\mathrm{Re}(z)| \Big\}.$$

The region $\mathcal{S}_\alpha$ has a simple representation given by

$$\mathcal{S}_\alpha = \left\{ \begin{array}{ll} z_0 \in \mathbb{C} : & \text{the IMEX DIMSIM is stable for any} \\ & z_1 = -|y|/\tan(\alpha) + iy, \ y \in \mathbb{R} \end{array} \right\}, \tag{2.5}$$

which follows from the maximum principle. For fixed values of $y \in \mathbb{R}$ we define also the sets

$$\mathcal{S}_{\alpha,y} = \left\{ \begin{array}{ll} z_0 \in \mathbb{C} : & \text{the IMEX DIMSIM is stable for fixed} \\ & z_1 = -|y|/\tan(\alpha) + iy \end{array} \right\}. \tag{2.6}$$

Observe that

$$\mathcal{S}_\alpha = \bigcap_{y \in \mathbb{R}} \mathcal{S}_{\alpha,y}. \tag{2.7}$$

The region $\mathcal{S}_{\alpha,0}$ is independent of $\alpha$, and corresponds to the region of absolute stability of the explicit method with coefficients $\mathbf{c}$, $\mathbf{A}$, $\mathbf{U}$, $\mathbf{B}$, and $\mathbf{V}$. This region will be denoted by $\mathcal{S}_E$. We have

$$\mathcal{S}_\alpha \subset \mathcal{S}_E, \tag{2.8}$$

and we will look for IMEX DIMSIMs for which the stability region $\mathcal{S}_\alpha$ contains a large part of the stability region $\mathcal{S}_E$ of the explicit method.

All these regions $\mathcal{S}_E$, $\mathcal{S}_{\alpha,y}$, and $\mathcal{S}_\alpha$, for fixed $y \in \mathbb{R}$ and $\alpha \in (0, \pi/2]$, can be determined by the algorithms developed in recent papers [12–14]. These algorithms are based on some variants of the boundary locus method to compute the boundaries $\partial\mathcal{S}_E$, $\partial\mathcal{S}_{\alpha,y}$, and $\partial\mathcal{S}_\alpha$, of the regions $\mathcal{S}_E$, $\mathcal{S}_{\alpha,y}$, and $\mathcal{S}_\alpha$. We refer to the papers [12–14] for a detailed description of these algorithms. The areas of $\mathcal{S}_E$ and $\mathcal{S}_\alpha$ can be computed by numerical integration in polar coordinates. We refer again to [12–14] for a detailed description of this process.

## 3. Construction of IMEX DIMSIMs with desirable stability properties

Examples of IMEX DIMSIMs of order $p = 1$, $p = 2$, $p = 3$, and $p = 4$ are given in [34,35,14]. In this section we will describe the construction of IMEX DIMSIMs of high order ($p = 5$ and $p = 6$) with $p = q = r = s$. The explicit and implicit parts of the IMEX scheme are defined by the same abscissa vector $\mathbf{c} = [c_1, \ldots, c_s]^T \in \mathbb{R}^s$, and coefficient matrices

$$\left[\begin{array}{c|c} \mathbf{A} & \mathbf{U} \\ \hline \mathbf{B} & \mathbf{V} \end{array}\right] \quad \text{and} \quad \left[\begin{array}{c|c} \widehat{\mathbf{A}} & \mathbf{U} \\ \hline \widehat{\mathbf{B}} & \mathbf{V} \end{array}\right],$$

where $\mathbf{U} = \mathbf{I}$, and the coefficient matrix $\mathbf{V}$ is a rank one matrix of the form $\mathbf{V} = \mathbf{e}\mathbf{v}^T$, with $\mathbf{e} = [1, \ldots, 1]^T \in \mathbb{R}^s$, $\mathbf{v} = [v_1, \ldots, v_s]^T \in \mathbb{R}^s$, and $\mathbf{v}^T\mathbf{e} = 1$, compare [9,23]. For given $\mathbf{A}$, $\widehat{\mathbf{A}}$, and $\mathbf{V}$, the explicit method, implicit method, and the IMEX scheme have order $p$ and stage order $q = p$ if the coefficient matrices $\mathbf{B}$ and $\widehat{\mathbf{B}}$ are computed from the relations

$$\mathbf{B} = \mathbf{B}_0 - \mathbf{A}\mathbf{B}_1 - \mathbf{V}\mathbf{B}_2 + \mathbf{V}\mathbf{A}, \quad \widehat{\mathbf{B}} = \mathbf{B}_0 - \widehat{\mathbf{A}}\mathbf{B}_1 - \mathbf{V}\mathbf{B}_2 + \mathbf{V}\widehat{\mathbf{A}}. \tag{3.1}$$

Here, $\mathbf{B}_0$, $\mathbf{B}_1$, and $\mathbf{B}_2$ are $s \times s$ matrices with the $(i, j)$ elements given by

$$\frac{\int_0^{1+c_i} \phi_j(x)dx}{\phi_j(c_j)}, \quad \frac{\phi_j(1+c_i)}{\phi_j(c_j)}, \quad \frac{\int_0^{c_i} \phi_j(x)dx}{\phi_j(c_j)},$$

$i, j = 1, 2, \ldots, s$, and $\phi_i(x) = \prod_{j=1, j\neq i}^{s}(x - c_j)$, $i = 1, 2, \ldots, s$, compare Th. 5.1 in [9] or Th. 3.2.1 in [23]. We will look for methods such that the implicit part of the scheme is $A(\alpha)$-stable for some $\alpha \in (0, \pi/2]$, $A$-, or $L$-stable, and the explicit part of the scheme has a large region of absolute stability. This will be done by solving the minimization problems

$$-\text{area}(\mathcal{S}_E) \longrightarrow \min, \tag{3.2}$$

or

$$-\text{area}(\mathcal{S}_\alpha) \longrightarrow \min, \tag{3.3}$$

for $\alpha \in (0, \pi/2]$, usually starting with many random guesses. However, even with extensive experience in optimization solving the above minimization problems and the determination of the IMEX methods of higher order is a real challenge. As already mentioned above, in this work the orders $p = 5$ and $p = 6$ are considered, and without the experience for the lower order, the higher one may well have been elusive. No sophisticated single algorithm could solve the problem. Global methods or hybrid approaches such as `multistart` in Matlab were not making any progress. The solution process was a combination of finding coefficients which correspond to a slightly larger area in (3.2) or (3.3) and a subsequent enlarging of this area. For both tasks derivative-free minimization methods were used, in particular `fminsearch` in Matlab. This function implements the Nelder–Mead method [27] which is also called the simplex method for unconstrained optimization. It yields, in general, only approximate local minima by deforming an initial simplex through reflection, shrinking, contraction, and expansion to a sufficiently small final simplex. However, it was demonstrated in [19], that convergence of this method is not guaranteed. These were compute-intensive procedures and multi-threaded computations on multi-core computers were useful in reducing the time needed.

In addition to the standard case of $\alpha = \pi/2$ we also found methods with considerably larger stability regions for $\alpha = \pi/4$. We could utilize the best coefficients found for $\alpha = \pi/2$ as starting values, thus substantially speeding up the computation.

The methods constructed in Section 3.1 and 3.2 were tested on some problems of the form (1.1) in Section 5. We can observe that the performance of the method of order $p = 6$ and stage order $q = p = 6$ with maximal area of $\mathcal{S}_{\pi/4}$ is not as good as of the scheme of the same order and the stage order corresponding to the maximal area of $\mathcal{S}_{\pi/2}$.

### 3.1. IMEX DIMSIMs with $p = q = r = s = 5$

Consider the IMEX DIMSIM (1.6) with abscissa vector $\mathbf{c}$ and coefficient matrices $\mathbf{A}$, $\mathbf{V}$, and $\widehat{\mathbf{A}}$ given by

$$\mathbf{c} = \begin{bmatrix} 0 \\ \frac{1}{4} \\ \frac{1}{2} \\ \frac{3}{4} \\ 1 \end{bmatrix}, \quad \mathbf{A} = \begin{bmatrix} 0 & 0 & 0 & 0 & 0 \\ a_{21} & 0 & 0 & 0 & 0 \\ a_{31} & a_{32} & 0 & 0 & 0 \\ a_{41} & a_{42} & a_{43} & 0 & 0 \\ a_{51} & a_{52} & a_{53} & a_{54} & 0 \end{bmatrix}, \quad \mathbf{V} = \mathbf{e}\mathbf{v}^T,$$

$$\mathbf{e} = \begin{bmatrix} 1 \\ 1 \\ 1 \\ 1 \\ 1 \end{bmatrix}, \quad \mathbf{v} = \begin{bmatrix} v_1 \\ v_2 \\ v_3 \\ v_4 \\ v_5 \end{bmatrix}, \quad \widehat{\mathbf{A}} = \begin{bmatrix} \lambda & 0 & 0 & 0 & 0 \\ \widehat{a}_{21} & \lambda & 0 & 0 & 0 \\ \widehat{a}_{31} & \widehat{a}_{32} & \lambda & 0 & 0 \\ \widehat{a}_{41} & \widehat{a}_{42} & \widehat{a}_{43} & \lambda & 0 \\ \widehat{a}_{51} & \widehat{a}_{52} & \widehat{a}_{53} & \widehat{a}_{54} & \lambda \end{bmatrix},$$

with

$$\begin{aligned} &\lambda = 0.2780538411364521, && \widehat{a}_{21} = 0.2204522761825798, \\ &\widehat{a}_{31} = 2.2948198957363657, && \widehat{a}_{32} = -0.6023667080712847, \\ &\widehat{a}_{41} = 5.0546209011538535, && \widehat{a}_{42} = -1.5298762183097632, \\ &\widehat{a}_{43} = 0.0971191414988231, && \widehat{a}_{51} = 9.3451677801081329, \\ &\widehat{a}_{52} = -1.4121335130997734, && \widehat{a}_{53} = -1.8834019985178697, \\ &\widehat{a}_{54} = 0.7825339554468704, \end{aligned}$$

$$\begin{aligned} &v_1 = -0.0793854651324349, && v_2 = 0.5543175729105773, \\ &v_3 = -1.5695895491441551, && v_4 = 2.3320745924436815, \\ &v_5 = 1 - v_1 - v_2 - v_3 - v_4, \end{aligned}$$

and the coefficient matrices $\mathbf{B}$ and $\widehat{\mathbf{B}}$ computed from (3.1). The stability polynomial of this IMEX scheme is

$$\begin{aligned} p(w, z_0, z_1) &= (1 - \lambda z_1)^5 w^5 - p_4(z_0, z_1) w^4 + p_3(z_0, z_1) w^3 \\ &- p_2(z_0, z_1) w^2 + p_1(z_0, z_1) w - p_0(z_0, z_1), \end{aligned}$$

where $p_4(z_0, z_1)$, $p_3(z_0, z_1)$, $p_2(z_0, z_1)$, $p_1(z_0, z_1)$, and $p_0(z_0, z_1)$, are polynomials of degree less than or equal to five. These polynomials depend also on the components of the coefficient matrix $\mathbf{A}$.

The implicit DIMSIM defined by $\mathbf{c}$, $\widehat{\mathbf{A}}$, $\widehat{\mathbf{B}}$, and $\mathbf{V}$ was derived in [10] (see also [23]), where it was also demonstrated that this method is $A$- and $L$-stable.

We have solved the minimization problems (3.2) and (3.3) in the parameter space $a_{21}$, $a_{31}$, $a_{32}$, $a_{41}$, $a_{42}$, $a_{43}$, $a_{51}$, $a_{52}$, $a_{53}$, and $a_{54}$ looking for methods with large regions of $\mathcal{S}_E$ and $\mathcal{S}_\alpha$ for $\alpha = \pi/2$. The solution to (3.2) leads to the method with parameters

$$\begin{aligned} &a_{21} = 0.5291120776096327, && a_{31} = 0.9663926557688088, \\ &a_{32} = 0.4205793801567606, && a_{41} = 0.0711934508983647, \\ &a_{42} = 0.2337212819719460, && a_{43} = 0.5195082185507158, \\ &a_{51} = 0.2935004666600090, && a_{52} = 0.9182698313383173, \\ &a_{53} = 0.6247434240189951, && a_{54} = 0.2562560329929151, \end{aligned}$$

for which the area of $\mathcal{S}_E$ is approximately equal to 5.86 and the area of $\mathcal{S}_{\pi/2}$ is approximately equal to 0.006. This method will be denoted by IMEX-DIMSIM5($\mathcal{S}_E$). We have plotted on Fig. 3.1 the boundaries of $\mathcal{S}_{\pi/2,y}$ for $y = -6.0, -5.4, \ldots, 6.0$ (thin lines), boundary of stability region $\mathcal{S}_E$ (thick line), and the stability region $\mathcal{S}_{\pi/2}$ (shaded region), where $-3.5 \le \mathrm{Re}(z_0) \le 0.5$ and $0 \le \mathrm{Im}(z_0) \le 1.5$ (top figure) and $-0.7 \le \mathrm{Re}(z_0) \le 0.1$ and $0 \le \mathrm{Im}(z_0) \le 0.2$ (bottom figure).

The solution to (3.3) with $\alpha = \pi/2$ leads to the method with parameters

$$\begin{aligned} &a_{21} = 0.4974348100506034, && a_{31} = -1.2241967653254258, \\ &a_{32} = 1.0540363795728771, && a_{41} = -1.6743539093452300, \\ &a_{42} = 1.6616796929302491, && a_{43} = 0.2774829129089688, \\ &a_{51} = 8.0587908598136835, && a_{52} = -0.3392227910111778, \\ &a_{53} = 1.4825037445366611, && a_{54} = -0.2486497791047641, \end{aligned}$$

for which the area of $\mathcal{S}_{\pi/2}$ is approximately equal to 0.99 and the area of $\mathcal{S}_E$ is approximately equal to 1.48. This method will be denoted by IMEX-DIMSIM5($\mathcal{S}_{\pi/2}$). We have plotted on Fig. 3.2 the boundaries of $\mathcal{S}_{\pi/2,y}$ for $y = -6.0, -5.4, \ldots, 6.0$ (thin lines), boundary of stability region $\mathcal{S}_E$ (thick line), and the stability region $\mathcal{S}_{\pi/2}$ (shaded region).

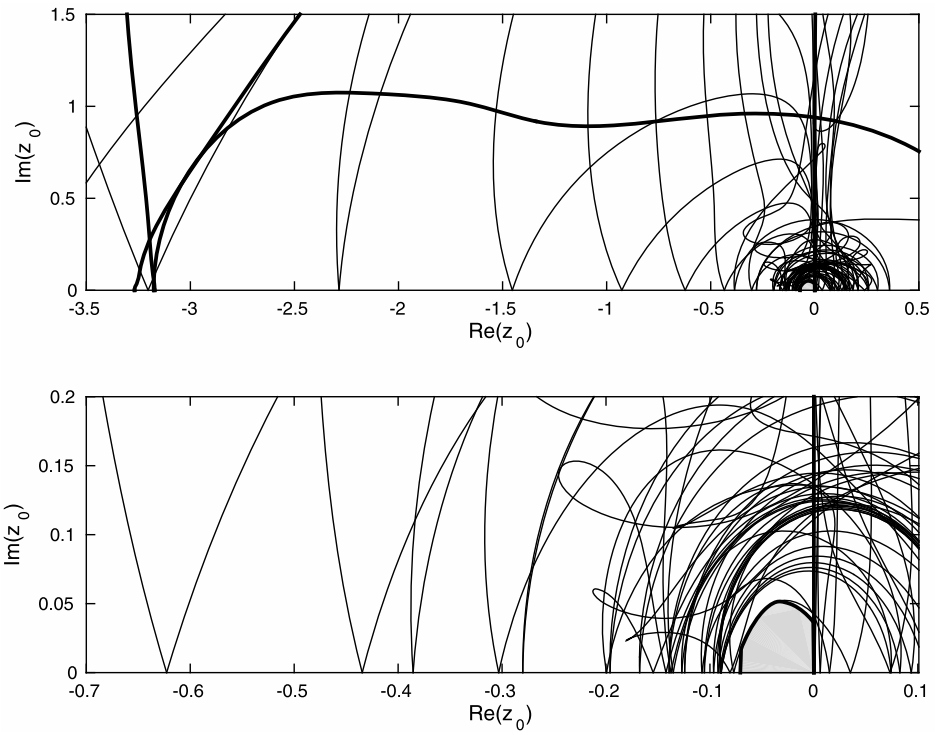


**Fig. 3.1.** Stability regions $\mathcal{S}_{\pi/2,y}$, $y = -6.0, -5.4, \ldots, 6.0$ (thin lines), $\mathcal{S}_{\pi/2}$ (shaded region) and $\mathcal{S}_E$ (thick line) for IMEX-DIMSIM5($\mathcal{S}_E$), where $-3.5 \le \mathrm{Re}(z_0) \le 0.5$ and $0 \le \mathrm{Im}(z_0) \le 1.5$ (top figure) and $-0.7 \le \mathrm{Re}(z_0) \le 0.1$ and $0 \le \mathrm{Im}(z_0) \le 0.2$ (bottom figure).

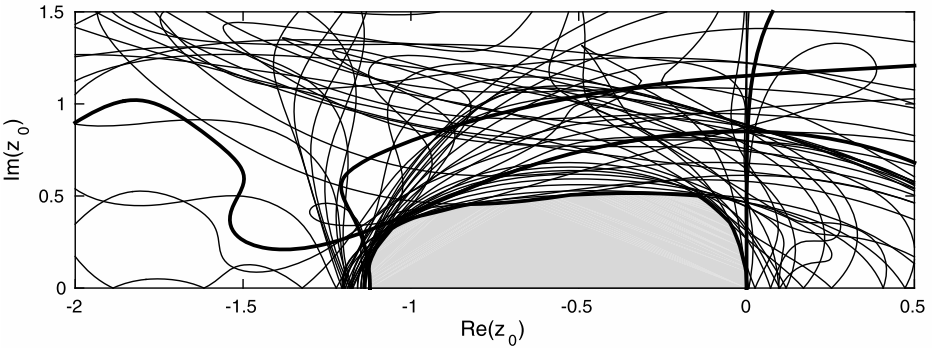


**Fig. 3.2.** Stability regions $\mathcal{S}_{\pi/2,y}$, $y = -6.0, -5.4, \ldots, 6.0$ (thin lines), $\mathcal{S}_{\pi/2}$ (shaded region) and $\mathcal{S}_E$ (thick line) for IMEX-DIMSIM5($\mathcal{S}_{\pi/2}$).

### 3.2. *IMEX DIMSIMs with* $p = q = r = s = 6$

Consider the IMEX DIMSIM (1.6) with abscissa vector $\mathbf{c}$ and coefficient matrices $\mathbf{A}$, $\mathbf{V}$, and $\widehat{\mathbf{A}}$ given by

$$\mathbf{c} = \begin{bmatrix} 0 \\ \frac{1}{5} \\ \frac{2}{5} \\ \frac{3}{5} \\ \frac{4}{5} \\ 1 \end{bmatrix}, \quad \mathbf{A} = \begin{bmatrix} 0 & 0 & 0 & 0 & 0 & 0 \\ a_{21} & 0 & 0 & 0 & 0 & 0 \\ a_{31} & a_{32} & 0 & 0 & 0 & 0 \\ a_{41} & a_{42} & a_{43} & 0 & 0 & 0 \\ a_{51} & a_{52} & a_{53} & a_{54} & 0 & 0 \\ a_{61} & a_{62} & a_{63} & a_{64} & a_{65} & 0 \end{bmatrix}, \quad \mathbf{V} = \mathbf{e}\mathbf{v}^T,$$

$$\mathbf{e}=\begin{bmatrix}1\\1\\1\\1\\1\\1\end{bmatrix},\quad \mathbf{v}=\begin{bmatrix}v_1\\v_2\\v_3\\v_4\\v_5\\v_6\end{bmatrix},\quad \widehat{\mathbf{A}}=\begin{bmatrix}\lambda & 0 & 0 & 0 & 0 & 0\\ \widehat{a}_{21} & \lambda & 0 & 0 & 0 & 0\\ \widehat{a}_{31} & \widehat{a}_{32} & \lambda & 0 & 0 & 0\\ \widehat{a}_{41} & \widehat{a}_{42} & \widehat{a}_{43} & \lambda & 0 & 0\\ \widehat{a}_{51} & \widehat{a}_{52} & \widehat{a}_{53} & \widehat{a}_{54} & \lambda & 0\\ \widehat{a}_{61} & \widehat{a}_{62} & \widehat{a}_{63} & \widehat{a}_{64} & \widehat{a}_{65} & \lambda\end{bmatrix},$$

with

$$\begin{aligned}
&\lambda = 0.334142367068050494, && \widehat{a}_{21} = 0.0440427826221396,\\
&\widehat{a}_{31} = 0.4315280967818837, && \widehat{a}_{32} = -0.6851178704555501,\\
&\widehat{a}_{41} = 0.1085855695963822, && \widehat{a}_{42} = -0.2677624797527218,\\
&\widehat{a}_{43} = -0.3834028421401898, && \widehat{a}_{51} = -1.8338525548076402,\\
&\widehat{a}_{52} = 2.8558219499708931, && \widehat{a}_{53} = -1.5734794843084787,\\
&\widehat{a}_{54} = 0.0399494641534270, && \widehat{a}_{61} = -5.6291661629969753,\\
&\widehat{a}_{62} = 11.9961113804644450, && \widehat{a}_{63} = -10.3776349045390960,\\
&\widehat{a}_{64} = 4.9832454380709700, && \widehat{a}_{65} = -1.1660323325876407,
\end{aligned}$$

$$\begin{aligned}
&v_1 = 2.1348868268276289, && v_2 = -9.9443804528196841,\\
&v_3 = 13.9345636860226090, && v_4 = 0.3296202234254039,\\
&v_5 = -14.6826061698900430, && v_6 = 1 - v_1 - v_2 - v_3 - v_4 - v_5,
\end{aligned}$$

and the coefficient matrices $\mathbf{B}$ and $\widehat{\mathbf{B}}$ computed from (3.1). The stability polynomial of this IMEX scheme is

$$\begin{aligned}
p(w, z_0, z_1) &= (1-\lambda z_1)^6 w^6 - p_5(z_0,z_1)\, w^5 + p_4(z_0,z_1)\, w^4 - p_3(z_0,z_1)\, w^3\\
&+ p_2(z_0,z_1)\, w^2 - p_1(z_0,z_1)\, w + p_0(z_0,z_1),
\end{aligned}$$

where $p_5(z_0,z_1)$, $p_4(z_0,z_1)$, $p_3(z_0,z_1)$, $p_2(z_0,z_1)$, $p_1(z_0,z_1)$, and $p_0(z_0,z_1)$, are polynomials of degree less than or equal to six. These polynomials depend also on the components of the coefficient matrix $\mathbf{A}$.

The implicit DIMSIM defined by $\mathbf{c}$, $\widehat{\mathbf{A}}$, $\widehat{\mathbf{B}}$, and $\mathbf{V}$ was derived in [10] (see also [23]), where it was also demonstrated that this method is $A$- and $L$-stable.

We have solved the minimization problems (3.2) and (3.3) in the parameter space $a_{21}$, $a_{31}$, $a_{32}$, $a_{41}$, $a_{42}$, $a_{43}$, $a_{51}$, $a_{52}$, $a_{53}$, $a_{54}$, $a_{61}$, $a_{62}$, $a_{63}$, $a_{64}$, and $a_{65}$, looking for methods with large regions of $\mathcal{S}_E$ and $\mathcal{S}_\alpha$ for $\alpha = \pi/2$ and $\alpha = \pi/4$. The solution to (3.2) leads to the method with parameters

$$\begin{aligned}
&a_{21} = -0.2900030317311283, && a_{31} = -0.1579123033624436,\\
&a_{32} = -0.2430974171717467, && a_{41} = -0.5385813131913196,\\
&a_{42} = 0.0146029415190869, && a_{43} = 0.1749447309819029,\\
&a_{51} = -0.1657106389572754, && a_{52} = -1.0959346712909215,\\
&a_{53} = 1.3954670319002449, && a_{54} = -0.0694602195754066,\\
&a_{61} = -0.2240144268106321, && a_{62} = 0.1741505226209945,\\
&a_{63} = -0.3923887577291381, && a_{64} = 0.1885799972582234,\\
&a_{65} = 0.3469082802087382,
\end{aligned}$$

for which the area of $\mathcal{S}_E$ is approximately equal to 0.28 and the area of $\mathcal{S}_{\pi/2}$ is approximately equal to 0.0002 only. This method will be denoted by IMEX-DIMSIM6($\mathcal{S}_E$). We have plotted on Fig. 3.3 the boundaries of $\mathcal{S}_{\pi/2,y}$ for $y = -8.0, -7.2, \ldots, 8.0$ (thin lines), boundary of stability region $\mathcal{S}_E$ (thick line), and the stability region $\mathcal{S}_{\pi/2}$ (small shaded region near the origin), where $-1 \le \mathrm{Re}(z_0) \le 0.5$ and $0 \le \mathrm{Im}(z_0) \le 1$ (top figure) and $-0.04 \le \mathrm{Re}(z_0) \le 0.02$ and $0 \le \mathrm{Im}(z_0) \le 0.04$ (bottom figure).

The solution to (3.3) with $\alpha = \pi/2$ leads to the method with parameters

$$\begin{aligned}
&a_{21} = 0.0632143552161613, && a_{31} = -0.5830149900613523,\\
&a_{32} = 0.8528243957842611, && a_{41} = -0.3141466024260616,\\
&a_{42} = 0.1889246726314440, && a_{43} = 0.5350461880358839,\\
&a_{51} = 0.5807888108797878, && a_{52} = -1.0434849901140222,\\
&a_{53} = 1.2395282097202411, && a_{54} = 0.1591739216110718,\\
&a_{61} = 1.1861133189790749, && a_{62} = -0.3432731372416638,\\
&a_{63} = -1.1744201836361277, && a_{64} = 1.6768301629926756,\\
&a_{65} = -0.0323827252087411,
\end{aligned}$$

for which the area of $\mathcal{S}_{\pi/2}$ is approximately equal to 0.082 and the area of $\mathcal{S}_E$ is approximately equal to 0.16. This method will be denoted by IMEX-DIMSIM6($\mathcal{S}_{\pi/2}$). We have plotted on Fig. 3.4 the boundaries of $\mathcal{S}_{\pi/2,y}$ for $y = -8.0, -7.2, \ldots, 8.0$ (thin lines), boundary of stability region $\mathcal{S}_E$ (thick line), and the stability region $\mathcal{S}_{\pi/2}$ (shaded region).

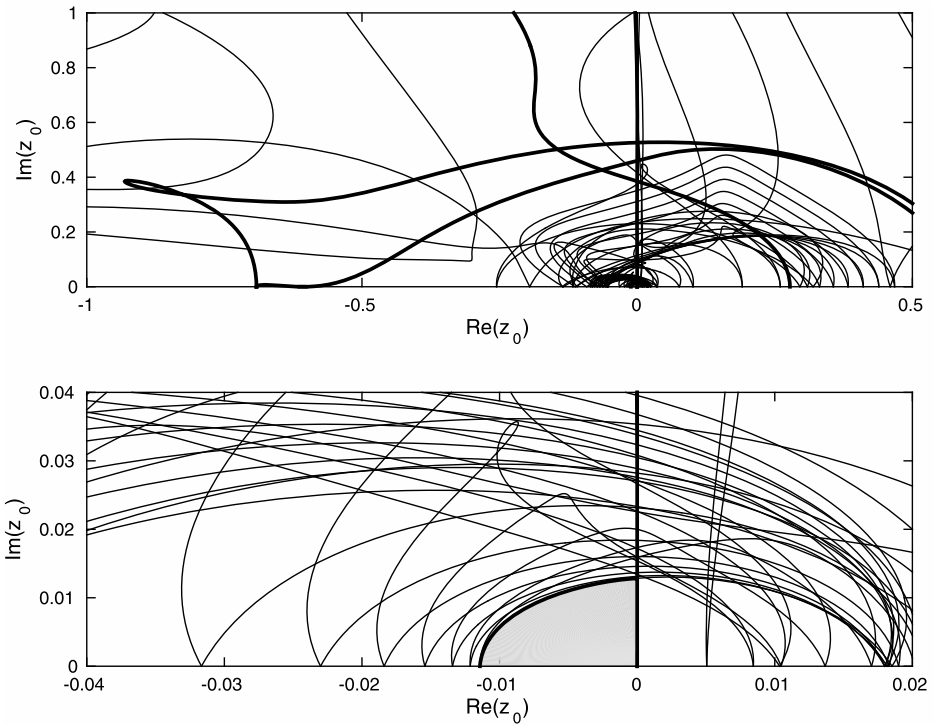


**Fig. 3.3.** Stability regions $\mathcal{S}_{\pi/2,y}$, $y = -8.0, -7.2, \ldots, 8.0$ (thin lines), $\mathcal{S}_{\pi/2}$ (small shaded region near the origin) and $\mathcal{S}_E$ (thick line) for IMEX-DIMSIM6($\mathcal{S}_E$), where $-1 \le \mathrm{Re}(z_0) \le 0.5$ and $0 \le \mathrm{Im}(z_0) \le 1$ (top figure) and $-0.04 \le \mathrm{Re}(z_0) \le 0.02$ and $0 \le \mathrm{Im}(z_0) \le 0.04$ (bottom figure).

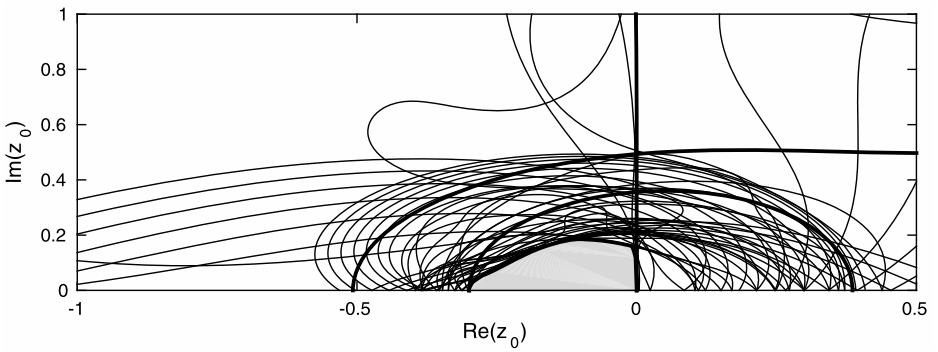


**Fig. 3.4.** Stability regions $\mathcal{S}_{\pi/2,y}$, $y = -8.0, -7.2, \ldots, 8.0$ (thin lines), $\mathcal{S}_{\pi/2}$ (shaded region) and $\mathcal{S}_E$ (thick line) for IMEX-DIMSIM6($\mathcal{S}_{\pi/2}$).

The solution to (3.3) with $\alpha = \pi/4$ leads to the method with parameters

$$
\begin{aligned}
a_{21} &= -0.0099313799873089, & a_{32} &= 0.8370512175514289,\\
a_{41} &= -0.3780901677281090, & a_{42} &= 0.3967716333487782,\\
a_{43} &= 0.5088123801911264, & a_{51} &= 0.7339314179584977,\\
a_{52} &= -1.6868641187748417, & a_{53} &= 1.7916558057718448,\\
a_{54} &= 0.0440789494145660, & a_{61} &= 0.8975019948816807,\\
a_{62} &= -0.6940821156051010, & a_{63} &= -0.1326190823857425,\\
a_{64} &= 1.4118953030148411, & a_{65} &= -0.0394329865721621,
\end{aligned}
$$

for which the area of $\mathcal{S}_{\pi/4}$ is approximately equal to 0.61 and the area of $\mathcal{S}_E$ is approximately equal to 0.75. This method will be denoted by IMEX-DIMSIM6($\mathcal{S}_{\pi/4}$). We have plotted on Fig. 3.5 the boundaries of $\mathcal{S}_{\pi/4,y}$ for $y = -8.0, -7.2, \ldots, 8.0$ (thin lines), boundary of stability region $\mathcal{S}_E$ (thick line), and the stability region $\mathcal{S}_{\pi/4}$ (shaded region).

Stability regions for IMEX DIMSIMs of order $1 \le p \le 4$ are plotted in [14], for extrapolated IMEX GLMs in [12], and for IMEX GLMs with inherent RK stability in [8]. Stability regions for IMEX RK methods are plotted are plotted in [13] and [22].

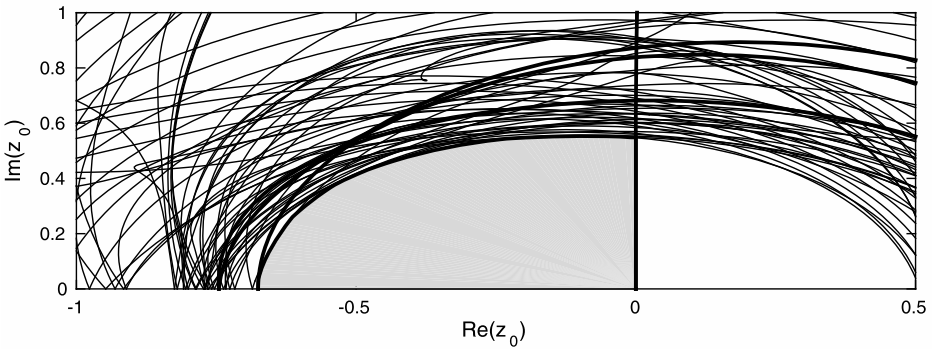


**Fig. 3.5.** Stability regions $\mathcal{S}_{\pi/4,y}$, $y = -8.0, -7.2, \ldots, 8.0$ (thin lines), $\mathcal{S}_{\pi/4}$ (shaded region) and $\mathcal{S}_E$ (thick line) for IMEX-DIMSIM6($\mathcal{S}_{\pi/4}$).

## 4. Starting and finishing procedures

To start the integration with IMEX DIMSIM (1.6) we have to compute the vector $y^{[0]} = x^{[0]} + z^{[0]}$, where

$$x_i^{[0]} = x(t_0) + \sum_{k=1}^{p} q_{ik} h^k x^{(k)}(t_0) + O(h^{p+1}), \quad i = 1, 2, \ldots, r,$$

$$z_i^{[0]} = z(t_0) + \sum_{k=1}^{p} \widehat{q}_{ik} h^k z^{(k)}(t_0) + O(h^{p+1}), \quad i = 1, 2, \ldots, r,$$

compare with (1.8). Since $x(t_0) + z(t_0) = y(t_0) = y_0$ this leads to

$$y_i^{[0]} = y_0 + \sum_{k=1}^{p} q_{ik} h^k x^{(k)}(t_0) + \sum_{k=1}^{p} \widehat{q}_{ik} h^k z^{(k)}(t_0) + O(h^{p+1}),$$

$i = 1, 2, \ldots, r$. Similarly as in [35], to compute approximations to $h^k u^{(k)}(t_0)$, $k = 1, 2, \ldots, p$, where $u = x$ or $u = z$, we will use the transformation

$$\begin{bmatrix} hu'(t_0) \\ hu'(t_1) \\ \vdots \\ hu'(t_{p-1}) \end{bmatrix} = (\mathbf{T} \otimes \mathbf{I}) \begin{bmatrix} hu'(t_0) \\ h^2 u''(t_0) \\ \vdots \\ h^p u^{(p)}(t_0) \end{bmatrix} + O(h^{p+1}),$$

where $\mathbf{I}$ is the identity matrix of dimension $m$, and the coefficients of the matrix $\mathbf{T}$ are computed by expanding $hu'(t_k)$, $k = 0, 1, \ldots, p-1$, into Taylor series around the point $t_0$. Then

$$\begin{bmatrix} hu'(t_0) \\ h^2 u''(t_0) \\ \vdots \\ h^p u^{(p)}(t_0) \end{bmatrix} = (\mathbf{S} \otimes \mathbf{I}) \begin{bmatrix} hu'(t_0) \\ hu'(t_1) \\ \vdots \\ hu'(t_{p-1}) \end{bmatrix} + O(h^{p+1}),$$

where $\mathbf{S} = \mathbf{T}^{-1}$. We then approximate $hx'(t_k) = hf(y(t_k))$ and $hz'(t_k) = hg(y(t_k))$ by $hf(y_k^{start})$ and $hg(y_k^{start})$, where $y_k^{start}$ are approximations to $y(t_k)$ computed by some self starting scheme, for example IMEX RK methods of order $p$.

It can be easily verified that for method of order $p = 5$ the matrix $\mathbf{S}$ is given by

$$\mathbf{S} = \begin{bmatrix} 1 & 0 & 0 & 0 & 0 \\ -\frac{25}{12} & 4 & -3 & \frac{4}{3} & -\frac{1}{4} \\ \frac{35}{12} & -\frac{26}{3} & \frac{19}{2} & -\frac{14}{3} & \frac{11}{12} \\ -\frac{5}{2} & 9 & -12 & 7 & -\frac{3}{2} \\ 1 & -4 & 6 & -4 & 1 \end{bmatrix},$$

and for methods of order $p = 6$ this matrix takes the form

$$\mathbf{S}=\begin{bmatrix} 1 & 0 & 0 & 0 & 0 & 0 \\ -\frac{137}{60} & 5 & -5 & \frac{10}{3} & -\frac{5}{4} & \frac{1}{5} \\ \frac{15}{4} & -\frac{77}{6} & \frac{107}{6} & -13 & \frac{61}{12} & -\frac{5}{6} \\ -\frac{17}{4} & \frac{71}{4} & -\frac{59}{2} & \frac{49}{2} & -\frac{41}{4} & \frac{7}{4} \\ 3 & -14 & 26 & -24 & 11 & -2 \\ -1 & 5 & -10 & 10 & -5 & 1 \end{bmatrix}.$$

We conclude this section with a short discussion of finishing procedure. Since all methods constructed in this paper have order $p$ and stage order $q=p$, and the last component of the abscissa vector $\mathbf{c}$ is equal to one ($c_s=1$), the approximation of order $p$ to the solution $y$ of (1.1) at the end point of the interval of integration $T$ is provided by the stage value $Y_s^{[N]}$, i.e., $Y_s^{[N]}=y(T)+O(h^p)$. The construction of finishing procedures for IMEX GLMs of order $p$ and stage order $q=p-1$ is discussed in [35].

## 5. Numerical experiments

In this section we will demonstrate that the methods constructed in this paper do not suffer from order reduction phenomenon which affects methods of low stage order such as, for example, IMEX RK methods [1,3,4].

Our first test problem is the famous van der Pol system

$$\begin{aligned} y_1' &= y_2, \\ y_2' &= \big((1-y_1^2)y_2-y_1\big)/\epsilon, \end{aligned} \tag{5.1}$$

$t\in[0,0.55139]$, where the first component is non-stiff and the second component is stiff for small values of the parameter $\epsilon$. The initial values are

$$y_1(0)=2, \quad y_2(0)=-\frac{2}{3}+\frac{10}{81}\epsilon-\frac{292}{2187}\epsilon^2-\frac{1814}{19683}\epsilon^3+O(\epsilon^4),$$

which, as observed in [3,26], do not produce initial transients, and as a result, the problem (5.1) is stiff on the whole interval of integration.

For the solution to the system (5.1) we have $y=[y_1,y_2]^T=x+z$, where $x=[y_1,0]^T$, $z=[0,y_2]^T$, and

$$x'=f(y)=[y_2,0]^T, \quad z'=g(y)=[0,((1-y_1^2)y_2-y_1)/\epsilon]^T.$$

The derivatives $x^{(k)}$ and $z^{(k)}$, $k=1,2,\dots,p$, can be computed exactly from the formulas

$$x^{(k)}=\begin{bmatrix} y_{k+1} \\ 0 \end{bmatrix}, \quad z^{(k)}=\begin{bmatrix} 0 \\ y_{k+2} \end{bmatrix}, \quad k=1,2,\dots,p,$$

where $y_3$, $y_4$, $y_5$, $y_6$, $y_7$, and $y_8$ can be determined from the recurrence relations

$$\begin{aligned} y_3 &= \big((1-y_1^2)y_2-y_1\big)/\epsilon, \\ y_4 &= \big((1-y_1^2)y_3-2y_1y_2^2-y_2\big)/\epsilon, \\ y_5 &= \big((1-y_1^2)y_4-6y_1y_2y_3-2y_2^3-y_3\big)/\epsilon, \\ y_6 &= \big((1-y_1^2)y_5-8y_1y_2y_4-12y_2^2y_3-6y_1y_3^2-y_4\big)/\epsilon, \\ y_7 &= \big((1-y_1^2)y_6-10y_1y_2y_5-20y_2^2y_4-30y_2y_3^2-20y_1y_3y_4-y_5\big)/\epsilon, \\ y_8 &= \big((1-y_1^2)y_7-12y_1y_2y_6-30y_2^2y_5-30y_1y_3y_5-30y_3^3-120y_2y_3y_4-20y_1y_4^2-y_6\big)/\epsilon, \end{aligned}$$

compare [11,8]. To solve the nonlinear systems of equations with respect to $Y_i^{[n+1]}$, resulting from the application of IMEX scheme (1.6) to (5.1), we have used the Newton method with the exact Jacobian of the function $g(y)$ given by

$$J_g(y)=\frac{\partial g}{\partial y}=\begin{bmatrix} \frac{\partial g_1}{\partial y_1} & \frac{\partial g_1}{\partial y_2} \\ \frac{\partial g_2}{\partial y_1} & \frac{\partial g_2}{\partial y_2} \end{bmatrix}=\begin{bmatrix} 0 & 0 \\ \frac{-2y_1y_2-1}{\epsilon} & \frac{1-y_1^2}{\epsilon} \end{bmatrix}.$$

The results of numerical experiments with the methods IMEX-DIMSIM5($\mathcal{S}_{\pi/2}$), IMEX-DIMSIM6($\mathcal{S}_{\pi/2}$) and IMEX-DIMSIM6($\mathcal{S}_{\pi/4}$) constructed in Section 3.1 and 3.2 are presented in Fig. 5.1, 5.2 and 5.3. We have also listed in Table 5.1 the $L_1$-norm of errors at the end point of the interval of integration and observed orders of convergence $p$ for IMEX-DIMSIM5($\mathcal{S}_{\pi/2}$), IMEX-DIMSIM6($\mathcal{S}_{\pi/2}$) and IMEX-DIMSIM6($\mathcal{S}_{\pi/4}$) applied to the van der Pol equation (5.1) with $\epsilon=10^{-6}$. We can see that all methods achieve the expected order of accuracy and that there is no order reduction for these IMEX schemes.

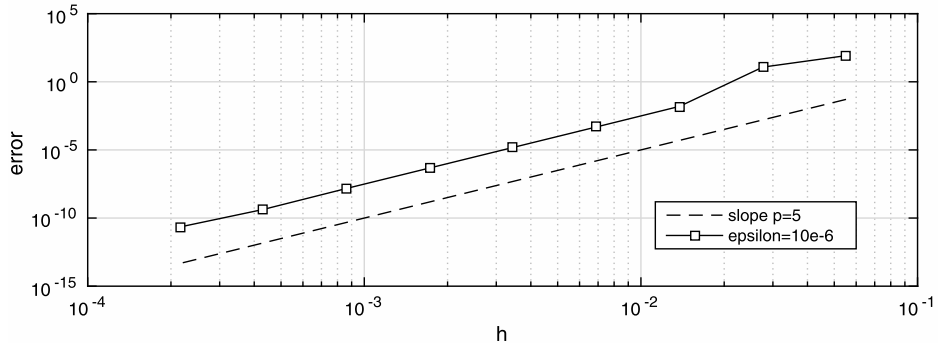


**Fig. 5.1.** Error versus stepsize for IMEX-DIMSIM5($\mathcal{S}_{\pi/2}$) of order $p=5$ and stage order $q=p=5$ applied to the van der Pol equation (5.1) with $\epsilon=10^{-6}$.

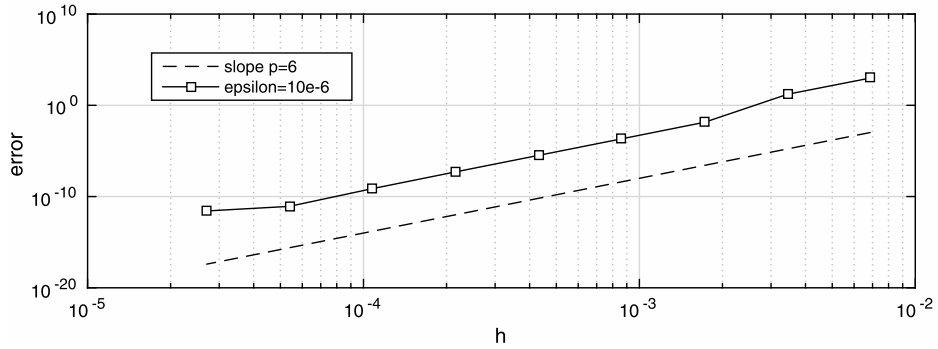


**Fig. 5.2.** Error versus stepsize for IMEX-DIMSIM6($\mathcal{S}_{\pi/2}$) of order $p=6$ and stage order $q=p=6$ applied to the van der Pol equation (5.1) with $\epsilon=10^{-6}$.

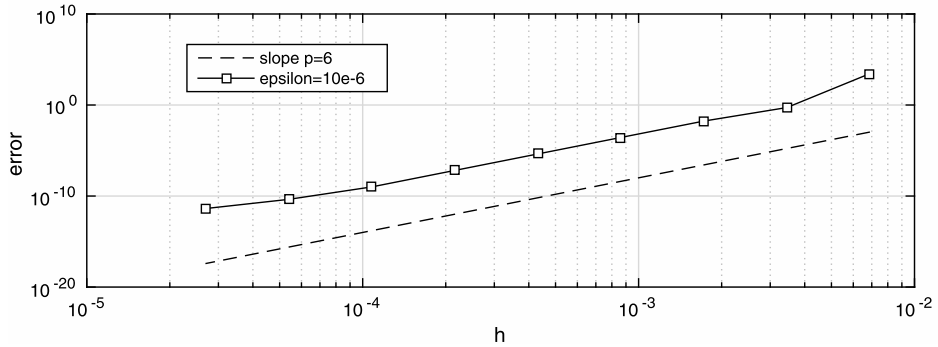


**Fig. 5.3.** Error versus stepsize for IMEX-DIMSIM6($\mathcal{S}_{\pi/4}$) of order $p=6$ and stage order $q=p=6$ applied to the van der Pol equation (5.1) with $\epsilon=10^{-6}$.

**Table 5.1**
$L_1$-norm of errors and observed orders of convergence $p$ for IMEX-DIMSIM5($\mathcal{S}_{\pi/2}$), IMEX-DIMSIM6($\mathcal{S}_{\pi/2}$) and IMEX-DIMSIM6($\mathcal{S}_{\pi/4}$) applied to the van der Pol equation (5.1) with $\epsilon=10^{-6}$.

| $h$ | IMEX-DIMSIM5($\mathcal{S}_{\pi/2}$) | | IMEX-DIMSIM6($\mathcal{S}_{\pi/2}$) | | IMEX-DIMSIM6($\mathcal{S}_{\pi/4}$) | |
|---|---|---|---|---|---|---|
| | $\|\text{error}\|_1$ | $p$ | $\|\text{error}\|_1$ | $p$ | $\|\text{error}\|_1$ | $p$ |
| 1.3785e−02 | 1.56e−02 | | | | | |
| 6.8924e−03 | 4.82e−04 | 5.02 | 9.93e+02 | | 2.81e+03 | |
| 3.4462e−03 | 1.52e−05 | 4.99 | 1.64e+01 | 5.92 | 5.27e−01 | 12.38 |
| 1.7231e−03 | 4.75e−07 | 5.00 | 1.39e−02 | 10.21 | 1.72e−02 | 4.94 |
| 8.6155e−04 | 1.48e−08 | 5.00 | 2.11e−04 | 6.04 | 2.70e−04 | 5.99 |
| 4.3077e−04 | 4.26e−10 | 5.12 | 3.27e−06 | 6.01 | 4.19e−06 | 6.01 |
| 2.1539e−04 | 2.21e−11 | 4.27 | 5.04e−08 | 6.02 | 6.44e−08 | 6.02 |
| 1.0769e−04 | | | 7.36e−10 | 6.10 | 1.00e−09 | 6.01 |
| 5.3847e−05 | | | 8.38e−12 | 6.46 | 4.29e−11 | 4.54 |

Our next example is the Brusselator system [18]

$$\begin{aligned}\frac{\partial u}{\partial t} &= A + u^2 v - (B+1)u + \alpha \frac{\partial^2 u}{\partial x^2},\\ \frac{\partial v}{\partial t} &= Bu - u^2 v + \alpha \frac{\partial^2 v}{\partial x^2},\end{aligned} \tag{5.2}$$

$0 \le x \le 1$, with initial conditions

$$u(x,0) = 1 + \sin(2\pi x), \quad v(x,0) = 3,$$

and boundary conditions

$$u(0,t) = u(1,t) = 1, \quad v(0,t) = v(1,t) = 3.$$

The parameter values are $A = 1$, $B = 3$, and $\alpha = 1/50$. As in [18] we approximated the second order spatial derivatives by central finite differences of the second order on the uniform grid $x_i = i\Delta x$, $i = 1, 2, \ldots, N$, where $\Delta x = 1/(N+1)$, $N = 100$. This leads to the system of $2N$ differential equations for the functions $u_i(t) \approx u(x_i, t)$ and $v_i(t) \approx v(x_i, t)$

$$\begin{aligned}u_i' &= A + u_i^2 v_i - (B+1)u_i + \frac{\alpha}{(\Delta x)^2}\Big(u_{i+1} - 2u_i + u_{i-1}\Big),\\ v_i' &= Bu_i - u_i^2 v_i + \frac{\alpha}{(\Delta x)^2}\Big(v_{i+1} - 2v_i + v_{i-1}\Big),\end{aligned} \tag{5.3}$$

$i = 1, 2, \ldots, N$, $u_0(t) = u_{N+1}(t) = 1$, $v_0(t) = v_{N+1}(t) = 3$, with initial conditions

$$u_i(0) = 1 + \sin(2\pi x_i), \quad v_i(0) = 3,$$

$i = 1, 2, \ldots, N$. Similarly as was done in [21] we treated the approximations to the diffusion terms in (5.3) by implicit methods and the reaction terms in (5.3) by explicit methods. The results of numerical experiments with IMEX-DIMSIM5($\mathcal{S}_{\pi/2}$), IMEX-DIMSIM6($\mathcal{S}_{\pi/2}$), and IMEX-DIMSIM6($\mathcal{S}_{\pi/4}$), are presented in Fig. 5.4, 5.5 and 5.6. We can observe again that all IMEX schemes achieve approximately the expected order of convergence, and that there is no order reduction for some range of stepsizes.

It is interesting to contrast this behavior of IMEX DIMSIMs constructed in this paper, for which there is no order reduction for some range of stepsizes, with the behavior of IMEX RK methods, for which some order reduction can be usually observed. We have applied to the system (5.3) IMEX RK methods of order $p = 4$ with $s = 8$ stages constructed in [22], which were obtained by maximizing the area($\mathcal{S}_\alpha$) for $\alpha = \pi/2$ of the explicit part of the IMEX RK scheme, assuming that the implicit part is $A$-stable. The resulting method obtained in this way is denoted by IMEX-RK48($\mathcal{S}_{\pi/2}$). For this scheme area($\mathcal{S}_E$) = 13.87 and area($\mathcal{S}_{\pi/2}$) = 11.02, and the corresponding stability regions are plotted in [22]. The results of numerical experiments with IMEX-RK48($\mathcal{S}_{\pi/2}$) are presented in Fig. 5.7. In contrast to IMEX DIMSIMs, we can observe order reduction for this scheme of order $p = 4$: the observed order of convergence is $p = 3$ for the same range of stepsizes as that used for IMEX-DIMSIM5($\mathcal{S}_{\pi/2}$).

We also consider the CUSP problem from [18]. This is a system of three PDEs which combine Zeeman's cusp catastrophe model for the nerve impulse mechanism [33] and the classical van der Pol oscillator. This problem takes the form

$$\begin{aligned}\frac{\partial y}{\partial t} &= -\frac{1}{\epsilon}\big(y^3 + ay + b\big) + \sigma \frac{\partial^2 y}{\partial x^2},\\ \frac{\partial a}{\partial t} &= b + 0.07v + \sigma \frac{\partial^2 a}{\partial x^2},\\ \frac{\partial a}{\partial t} &= (1 - a^2)b - a - 0.4y + 0.035v + \sigma \frac{\partial^2 b}{\partial x^2},\end{aligned} \tag{5.4}$$

$0 \le x \le 1$, $t \in [0, t_{end}]$, where $v = u/(u + 0.1)$, $u = (y - 0.7)(y - 1.3)$. As in [18] we choose $\alpha = 1/144$ and $\epsilon = 10^{-4}$. This problem is discretized by the method of lines on the uniform grid $x_i = i\Delta x$, $i = 0, 1, \ldots, N$, $N\Delta x = 1$, which leads to a large system of ODES with periodic boundary conditions and appropriate initial conditions, compare [18]. As in [18] we choose $N = 32$ and $t_{end} = 1.1$. The stiffness in this problem comes from a small parameter $\epsilon$ and the discretization of the diffusion terms $\partial^2 y/\partial x^2$, $\partial^2 a/\partial x^2$, $\partial^2 b/\partial x^2$. The IMEX scheme treats the stiff terms in the resulting system of ODEs by the implicit method and the remaining terms by the explicit method. The results of numerical experiments with IMEX-DIMSIM5($\mathcal{S}_{\pi/2}$), are presented on Fig. 5.8. The average observed order of convergence for the range of stepsizes $10^{-4} \le h \le 7.8125 \cdot 10^{-7}$ is $p = 5.19$. The behavior of error is not as regular for IMEX-DIMSIM6($\mathcal{S}_{\pi/2}$), and IMEX-DIMSIM6($\mathcal{S}_{\pi/4}$), but the average observed orders of convergence for the range of stepsizes $10^{-4} \le h \le 1.5625 \cdot 10^{-6}$ are $p = 6.17$ and $p = 6.18$, respectively. In contrast, there is again order reduction for IMEX RK methods. The results of numerical experiments with IMEX-RK48($\mathcal{S}_{\pi/2}$) are presented on Fig. 5.9, and the average observed order of convergence for the range of stepsizes $10^{-4} \le h \le 7.8125 \cdot 10^{-7}$ is $p = 2.93$.

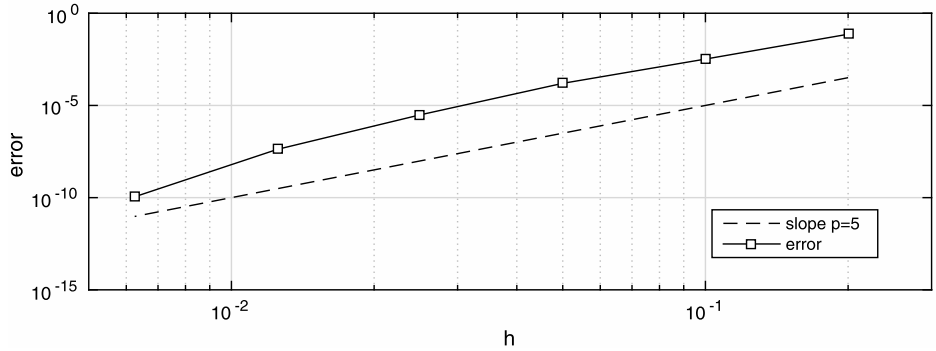


**Fig. 5.4.** Error versus stepsize for IMEX-DIMSIM5($\mathcal{S}_{\pi/2}$) of order $p = 5$ and stage order $q = p = 5$ applied to the discretization of the Brusselator system (5.3).

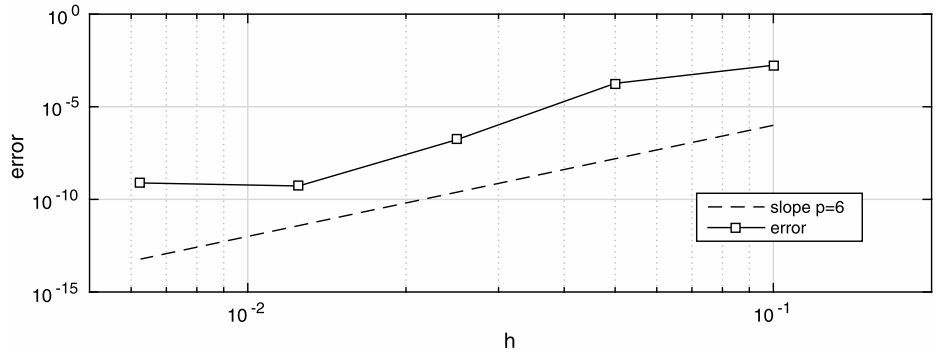


**Fig. 5.5.** Error versus stepsize for IMEX-DIMSIM6($\mathcal{S}_{\pi/2}$) of order $p = 6$ and stage order $q = p = 6$ applied to the discretization of the Brusselator system (5.3).

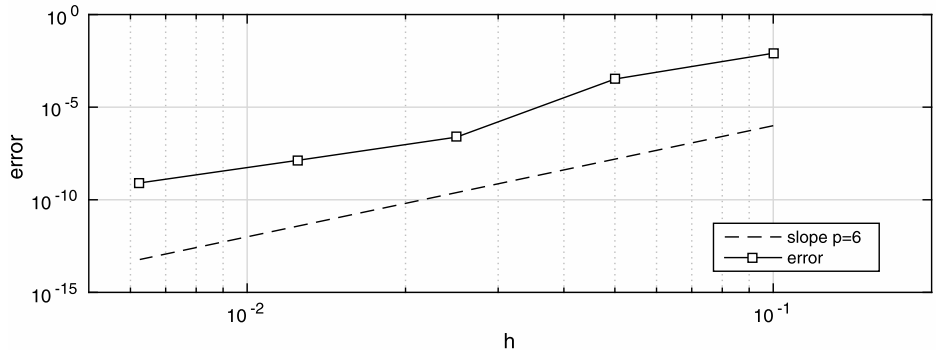


**Fig. 5.6.** Error versus stepsize for IMEX-DIMSIM6($\mathcal{S}_{\pi/4}$) of order $p = 6$ and stage order $q = p = 6$ applied to the discretization of the Brusselator system (5.3).

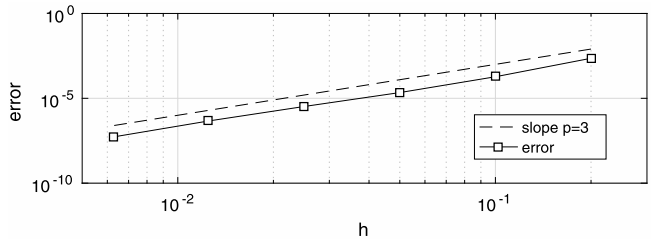


**Fig. 5.7.** Error versus stepsize for IMEX-RK48($\mathcal{S}_{\pi/2}$) of order $p = 4$ with $s = 8$ stages applied to the discretization of the Brusselator system (5.3).

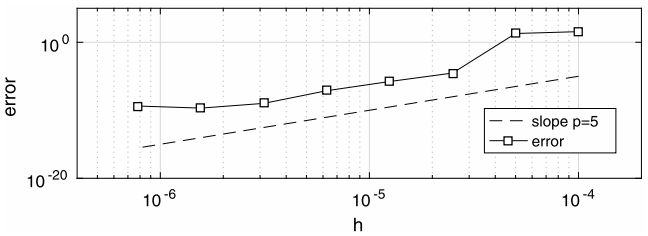


**Fig. 5.8.** Error versus stepsize for IMEX-DIMSIM5($\mathcal{S}_{\pi/2}$) applied to the discretization of CUSP problem (5.4).

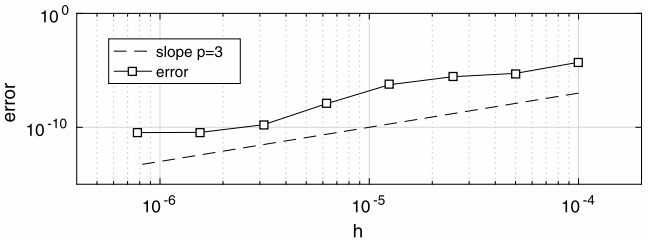


**Fig. 5.9.** Error versus stepsize for IMEX-RK48($\mathcal{S}_{\pi/2}$) of order $p = 4$ with $s = 8$ stages applied to the discretization of CUSP problem (5.4).

## 6. Concluding remarks

In this paper we constructed IMEX DIMSIMS of order $p = 5$ and $p = 6$ and stage order $q = p$. It was demonstrated by some numerical experiments that these schemes do not suffer from order reduction. This is in contrast to some IMEX RK methods considered in the literature on the subject.

The key to obtaining the results of this paper was the successful application of a rather specific optimization strategy. The well-known Nelder–Mead or simplex method cannot be shown to converge except in very special and low-dimensional situations. It was nevertheless the method which, when applied in a frequently restarted form and alternating between two different implementations, did yield the stability regions which, although at first appearing limited in size, allowed to demonstrate high orders for realistic stepsizes. In the light of these novel and very satisfactory results no statements need to be made about the definite possibility that the solutions were local and not necessarily global solutions.

Future work will address various implementation issues related to IMEX schemes, such as choice of initial stepsize, estimation of local discretization errors, construction of continuous extensions, and design of appropriate step size and order changing strategies.

## Acknowledgements

The authors wish to express their gratitude to the anonymous referees, whose comments helped to improve the presentation of this paper.

## References

[1] U.M. Asher, S.J. Ruuth, R.J. Spiteri, Implicit–explicit Runge–Kutta methods for time-dependent partial differential equations, Appl. Numer. Math. 25 (1997) 151–167.
[2] U.M. Asher, S.J. Ruuth, B. Wetton, Implicit–explicit methods for time dependent PDE's, SIAM J. Numer. Anal. 32 (1995) 797–823.
[3] S. Boscarino, Error analysis of IMEX Runge–Kutta methods derived from differential-algebraic systems, SIAM J. Numer. Anal. 45 (2007) 1600–1621 (electronic).
[4] S. Boscarino, On an accurate third order implicit–explicit Runge–Kutta method for stiff problems, Appl. Numer. Math. 59 (2009) 1515–1528.
[5] S. Boscarino, R. Bürger, P. Mulet, G. Russo, L. Villada, Linearly implicit IMEX Runge–Kutta methods for a class of degenerate convection–diffusion problems, SIAM J. Sci. Comput. 37 (2015) B305–B331.
[6] S. Boscarino, L. Pareschi, G. Russo, Implicit–explicit Runge–Kutta schemes for hyperbolic systems and kinetic equations in the diffusion limit, SIAM J. Sci. Comput. 35 (2013) A22–A51.
[7] S. Boscarino, G. Russo, Flux-explicit IMEX Runge–Kutta schemes for hyperbolic to parabolic relaxation problems, SIAM J. Numer. Anal. 51 (2013) 163–190.
[8] M. Braś, G. Izzo, Z. Jackiewicz, Accurate implicit–explicit general linear methods with inherent Runge–Kutta stability, J. Sci. Comput. 70 (2017) 1105–1143.
[9] J.C. Butcher, Diagonally-implicit multi-stage integration methods, Appl. Numer. Math. 11 (1993) 347–363.
[10] J.C. Butcher, Z. Jackiewicz, Construction of high order diagonally implicit multistage integration methods for ordinary differential equations, Appl. Numer. Math. 27 (1998) 1–12.
[11] J.C. Butcher, Z. Jackiewicz, W.M. Wright, Error propagation for general linear methods for ordinary differential equations, J. Complex. 23 (2007) 560–580.
[12] A. Cardone, Z. Jackiewicz, A. Sandu, H. Zhang, Extrapolation-based implicit–explicit general linear methods, Numer. Algorithms 65 (2014) 377–399.
[13] A. Cardone, Z. Jackiewicz, A. Sandu, H. Zhang, Extrapolated implicit–explicit Runge–Kutta methods, Math. Model. Anal. 19 (2014) 18–43.

[14] A. Cardone, Z. Jackiewicz, A. Sandu, H. Zhang, Construction of highly stable implicit–explicit general linear methods, in: Dynamical Systems, Differential Equations and Applications, 10th AIMS Conference. Suppl., Discrete Contin. Dyn. Syst. (2015) 185–194.
[15] M. Crouzeix, Une méthode multipas implicite–explicite pour l'approximation des équations d'évolution paraboliques, Numer. Math. 35 (1980) 257–276.
[16] J. Frank, W. Hundsdorfer, J.G. Verwer, On the stability of implicit–explicit linear multistep methods, Appl. Numer. Math. 25 (1997) 193–205.
[17] B. García-Celayeta, I. Higueras, T. Roldán, Contractivity/monotonicity for additive Runge–Kutta methods: inner product norms, Appl. Numer. Math. 56 (2006) 862–878.
[18] E. Hairer, G. Wanner, Solving Ordinary Differential Equations II. Stiff and Differential-Algebraic Problems, Springer Verlag, Berlin, Heidelberg, New York, 1996.
[19] N.J. Higham, Optimization by direct search in matrix computations, SIAM J. Matrix Anal. Appl. 14 (1993) 317–333.
[20] W. Hundsdorfer, S.J. Ruuth, IMEX extensions of linear multistep methods with general monotonicity and boundedness properties, J. Comput. Phys. 225 (2007) 2016–2042.
[21] W. Hundsdorfer, J.G. Verwer, Numerical Solution of Time-Dependent Advection–Diffusion–Reaction Equations, Springer-Verlag, Berlin, Heidelberg, New York, 2003.
[22] G. Izzo, Z. Jackiewicz, Highly stable implicit–explicit Runge–Kutta methods, Appl. Numer. Math. 113 (2017) 71–92.
[23] Z. Jackiewicz, General Linear Methods for Ordinary Differential Equations, John Wiley, Hoboken, New Jersey, 2009.
[24] C.A. Kennedy, M.H. Carpenter, Additive Runge–Kutta Schemes for Convection–Diffusion–Reaction Equations, Report NASA/TM-2001-211038, Langley Research Center, Hampton, Virginia, 2001.
[25] C.A. Kennedy, M.H. Carpenter, Additive Runge–Kutta schemes for convection–diffusion–reaction equations, Appl. Numer. Math. 44 (2003) 139–181.
[26] A.T. Layton, M.L. Minion, Implications of the choice of quadrature nodes for Picard integral deferred correction methods for ordinary differential equations, BIT 45 (2005) 341–373.
[27] J.A. Nelder, R. Mead, A simplex method for function minimization, Comput. J. 7 (1965) 308–313.
[28] L. Pareshi, G. Russo, Implicit–explicit Runge–Kutta schemes for stiff systems of differential equations, in: Recent Trends in Numerical Analysis, in: Adv. Theory Comput. Math., vol. 3, Nova Sci. Publ., Huntington, NY, 2001, pp. 269–288.
[29] L. Pareshi, G. Russo, Implicit–explicit Runge–Kutta schemes and applications to hyperbolic systems with relaxation, J. Sci. Comput. 25 (2005) 129–155.
[30] S.J. Ruuth, Implicit–explicit methods for reaction–diffusion problems in pattern formation, J. Math. Biol. 34 (1995) 148–176.
[31] J.M. Varah, Stability restrictions on second order, three-level finite-difference schemes for parabolic equations, SIAM J. Numer. Anal. 17 (1980) 300–309.
[32] D. Wang, S.J. Ruuth, Variable step-size implicit–explicit linear multistep methods for time-dependent partial differential equations, J. Comput. Math. 26 (2008) 838–855.
[33] E.C. Zeeman, Catastrophe Theory, Selected Papers, Addison-Wesley Publishing Co., Reading, Mass.–London–Amsterdam, 1977, pp. 1972–1977.
[34] H. Zhang, A. Sandu, A second-order diagonally-implicit multi-stage integration method, Proc. Comput. Sci. 9 (2012) 1039–1046.
[35] H. Zhang, A. Sandu, S. Blaise, Partitioned and implicit–explicit general linear methods for ordinary differential equations, J. Sci. Comput. 61 (2014) 119–144.
[36] E. Zharovsky, A. Sandu, H. Zhang, A class of implicit–explicit two-step Runge–Kutta methods, SIAM J. Numer. Anal. 53 (2015) 321–341.
[37] X. Zhong, Additive semi-implicit Runge–Kutta methods for computing high-speed nonequilibrium reactive flows, J. Comput. Phys. 128 (1996) 19–31.